REGULAR ARTICLE

Excess vibrational modes of a crystal in an external non-affine field[†]

SASWATI GANGULY[a] and SURAJIT SENGUPTA[b,*]

[a]Institut für Theoretische Physik II: Weiche Materie, Heinrich Heine-Universität Düsseldorf, Universitätsstraße 1, 40225 Düsseldorf, Germany
[b]TIFR Centre for Interdisciplinary Sciences, 21 Brundavan Colony, Narsingi, Hyderabad, Telangana 500 075, India
E-mail: surajit@tifrh.res.in

Abstract.   Thermal displacement fluctuations in a crystal may be classified as either "affine" or "non-affine". While the former couples to external stress with familiar consequences, the response of a crystal when *non-affine* displacements are enhanced using the thermodynamically conjugate field, is relatively less studied. We examine this using a simple model of a crystal in two dimensions for which analytical calculations are possible. Enhancing non-affine fluctuations destabilises the crystal. The population of small frequency phonon modes increases, with the phonon density of states shifting, as a whole, towards zero frequency. Even though the crystal is free of disorder, we observe growing length and time scales. Our results, which may have implications for the glass transition and structural phase transitions in solids, are compared to molecular dynamics simulations. Possibility of experimental verification of these results is also discussed.

Keywords.   Non-affine displacements; boson peak; vibrational density of states.

1. Introduction

While an ideal crystal is homogeneous at all length scales larger than the unit cell,[1] a defining characteristic of glasses is the presence of structural and dynamic heterogeneities.[2–5] Such heterogeneities, cause "soft spots",[6] participate in mechanical deformation,[7,8] and contribute to localised transverse vibrational modes.[9] They have been argued to also give rise to phenomenon of "boson peak",[10–13] viz., an enhancement in the weight of low frequency region in the phonon density of states. On the other hand, there are suggestions that the boson peak is unrelated to specific soft spots but simply represents an usual crystalline van Hove singularity broadened by disorder.[14–16] Indeed, explicit calculations for a model disordered solid shows that hybridisation of crystalline vibrational states and a shifting of the lowest van Hove singularity to the low frequency region due to disorder contributes to the boson peak phenomenon.[16]

This paper is an attempt to reconcile these two, seemingly divergent viewpoints. Our argument proceeds as follows. Soft spots, detected in computer simulations,[6,8] and in experiments on colloidal glasses,[12] undergo local

structural rearrangements during shear deformation.[17] These rearrangements are non-affine in the sense that they cannot be represented as an elastic strain on a reference volume.[8] We have shown,[18–20] that thermal fluctuations can cause non-affine displacements even in a homogeneous crystal. In this case, such deformations are, however, transient and are predominantly defect (dislocation pair) precursors.[21] We have also shown that it is possible to enhance (or suppress) these fluctuations in a crystal using an external field.[19] In this paper we ask what effect, if any, do these field enhanced non-affine deformations have on the phonon density of states of crystals?

To answer this question we consider a very simple crystal consisting of particles connected by harmonic bonds and arranged in a two dimensional triangular lattice.[22] While we ignore anharmonic effects, we demonstrate below that the model is still capable of showing non-trivial behaviour. A great advantage of this model, on the other hand, is the fact that many results may be obtained analytically,[18,19] completely removing artefacts arising from systematic and random errors from computer simulations or experiments.

Using the well defined projection formalism, which we have established in a previous publication,[18] we separate thermal particle displacements into affine and

non-affine subspaces. An external field is introduced,[19] which couples selectively only to the non-affine component of the displacements. The phonon dispersion curve and the density of states is then obtained as a function of the field. As the field is increased, vibrational modes at the Brillouin zone boundary becomes soft and the density of states gets enhanced in the low frequency region.[23] The smallest van Hove singularity, which appears as a sharp peak also shifts to the low frequency region. As a corollary, we show that this shift is accompanied by a many-fold increase in the correlation length and relaxation time of non-affine displacements.

Our results demonstrate, for what we believe to be the first time, that non-affine fluctuations are the primary cause for the boson peak phenomenon. These fluctuations are predominant in a disordered solid but can also be artificially tuned in an ordered crystal which, nevertheless remains perfectly homogeneous over large length and time scales. Disorder can broaden this response, which, again, we show explicitly by introducing random interactions in our model.

The rest of the paper is organised as follows. In the next section we explain the projection formalism for obtaining non-affine displacements and define our model system and simulation procedure to test our results. This is followed by a description of our main (analytic) results which are compared to simulations together with a discussion on the role of disorder. We end the paper with a summary of our main results and conclusions.

2. Non-Affine Fluctuations

An ideal crystal at a temperature $T \neq 0$ is a rather well understood object - its physics being completely specified by lattice vibrations.[23] The magnitude of lattice vibrations is often used as a measure to determine the stability of a crystal and its melting properties.[24]

For the special case of a *harmonic* crystal, defined, for example by the Hamiltonian,

$$\mathcal{H}_0 = \sum_{i=1}^{N} \frac{\mathbf{p}_i^2}{2m} + \frac{K}{2} \sum_{i=1}^{N} \sum_{j \in \Omega, i < j} (|\mathbf{r}_j - \mathbf{r}_i| - |\mathbf{R}_j - \mathbf{R}_i|)^2$$

$$(1)$$

many essential thermodynamic quantities may be obtained exactly. Here $\mathbf{p}_i$ the momentum, m the mass, $\mathbf{r}_i$ the instantaneous position, and $\mathbf{R}_i$ the reference position of particle i. The length scale is set by the lattice parameter l, the energy scale by Kl^2, and the time scale by $\sqrt{m/K}$. We have chosen $l = m = K = 1$. A dimensionless inverse temperature is given by $\beta = Kl^2/k_BT$, with k_B the Boltzmann constant. The interactions have a range equal to the size of Ω - a typical coordination volume.

In Refs.[18] and [19] we have described in detail how particle displacements in such a system may be projected onto affine strains and non-affine displacement components. While Ref.[18] gave the general theory and specific examples of the one dimensional chain and the two dimensional triangular lattice, Ref.[20] extended this formalism to the two dimensional honey-comb structure. Below, we give a brief summary of this procedure for completeness. While our procedure is perfectly general and can be carried through for any lattice in any dimension, we present results only for the two dimensional ($d = 2$) triangular lattice with Ω restricted to the first neighbour shell consisting of a central particle and its six neighbours.

Within Ω, around particle i, define relative atomic displacements, $\Delta_j = \mathbf{u}_j - \mathbf{u}_i$ with $j \neq i \in \Omega$. To obtain the best fit local affine deformation D, one minimises $\sum_j [\Delta_j - \mathsf{D}(\mathbf{R}_j - \mathbf{R}_i)]^2$ with the non-affinity parameter $\chi(\mathbf{R}_i) > 0$ given by the minimum value of this quantity.[8] In Ref.[18] we showed that this minimisation procedure is equivalent to a projection of Δ_i onto a non-affine subspace defined by the projection operators P, where $\chi(\mathbf{R}_i) = \Delta^{\mathrm{T}}\mathsf{P}\Delta$ and Δ is a column vector constructed out of the Δ_i. The projection operator $\mathsf{P}^2 = \mathsf{P} = \mathsf{I} - \mathsf{R}(\mathsf{R}^{\mathrm{T}}\mathsf{R})^{-1}\mathsf{R}^{\mathrm{T}}$ and $\mathsf{R}_{j\alpha,\gamma\gamma'} = \delta_{\alpha\gamma}R_{j\gamma'}$, with the central particle i taken to be at the origin.

In Ref.[18], we showed how the statistics of χ may be obtained for (1). For instance, the thermal average $\langle \chi \rangle$ is given by the sum of the eigenvalues, $\sum_\mu \sigma_\mu$, of PCP with $C_{i\alpha,j\gamma} = \langle \Delta_{i\alpha}\Delta_{j\gamma} \rangle$, the covariance matrix of the *coarse-grained* displacements. Using rather standard statistical mechanical techniques,[18,19] and appropriate generating functions, one can obtain explicitly both the single point probability, $P(\chi)$, and two point, spatio-temporal correlation function

$$C_\chi(\mathbf{R}, t) = \frac{\langle \chi(0,0)\chi(\mathbf{R}, t) \rangle - \langle \chi \rangle^2}{\langle \chi^2 \rangle - \langle \chi \rangle^2}.$$

These results are accurate for any solid at low temperatures and high densities where the harmonic approximation, used in deriving them, is valid.

The thermal average $\langle \chi \rangle$ for a crystalline solid is non-zero at any finite temperature, it is also, on the average, exponentially correlated in space and time with the spatial and temporal scales being set by the lattice parameter and the microscopic relaxation time. However, as we show below it is possible to enhance the expectation value and correlation of χ. We use a device introduced in Ref.[19] for this purpose.

Consider then the extended Hamiltonian,

$$\mathcal{H} = \mathcal{H}_0 - h_X \sum_i \sum_{jk \in \Omega} (\mathbf{u}_j - \mathbf{u}_i)^{\mathrm{T}}\mathbf{P}_{j-i,k-i}(\mathbf{u}_k - \mathbf{u}_i). \quad (2)$$

The term multiplying h_X involves the elements of the projection operator $\mathbf{P}_{ij}$, a function only of the reference configuration, that acts on particle displacements. Note that the extra term in (2) can also be represented as $h_X X$ where $X = \sum_i^N \chi(\mathbf{R}_i)$, the spatial average of the non-affine parameter χ. A positive value of the non-affine field h_X enhances non-affine distortions of the lattice,[18,19] namely, fluctuations
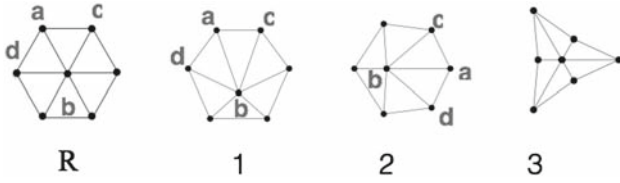
Figure 1. Non-affine distortions of the reference configuration **R**. The configurations 1 and 2 represent (degenerate) eigenvectors of PCP^T corresponding to the two largest eigenvalues σ_1 and σ_2. The next largest eigenvalue belongs to the eigenvector $\mu = 3$. Note that $\mu = 1$ and 2 represent distortions where nearest neighbours a, b move away from each other while next nearest neighbours c, d come closer tending to nucleate a dislocation dipole.[19] The third eigenvector represents coming together of 4 particles to form a triangular lattice of tetramers with twice the lattice parameter.

in particle positions projected onto a subspace spanned by the eigenvectors associated with the non-affine eigenvalues σ_μ. It is important to note that this new term does not break translational symmetry of the lattice. Indeed, the substitution $\mathbf{u}_i \rightarrow \mathbf{u}_i + \mathbf{c}$, for all particles i with $\mathbf{c}$ being an arbitrary constant displacement, keeps the Hamiltonian invariant.

Taking Ω as the nearest neighbour shell consisting of particle i and its 6 neighbours, we obtain 12 possible lattice modes. There are $d \times d = 4$ affine distortions in two dimensions, viz. local volume, uniaxial and shear distortion of Ω together with local rotations. The remaining 8 modes are non-affine and appear as non-trivial eigenvectors of PCP. The distribution of the eigenvalues is not uniform with the lowest eigenvalues being separated from the rest by a large gap.[19,20] In Figure 1, we have plotted three of the softest non-affine modes which have the highest eigenvalues and therefore make the largest contribution to χ. Note that the reciprocal of the eigenvalue is proportional to the curvature of the Hessian projected in the direction of the eigenvector. The two largest eigen-distortions, ($\mu = 1, 2$) are degenerate and have been shown to represent fluctuations which tend to nucleate a dislocation dipole. The third eigenvector ($\mu = 3$), with an eigenvalue about five times smaller, represents a fluctuation where the original triangular lattice transforms to another similar triangular structure consisting of tetramers with double the lattice parameter – similar to a period doubling transition commonly observed in one dimension.[1] The remaining higher energy modes represent more complicated distortions of Ω.

Analytic calculations of correlation functions for the model solid presented in the next section have been carried out using

Simulation results report molecular dynamics (MD) calculations.[25] MD simulations in the canonical ensemble, i.e., at constant particle number N, volume V and temperature T, were done using a leapfrog algorithm, coupling the system to a Brown and Clarke thermostat.[25] The size of the systems ranges from from $N = 100$ to $N = 40000$ particles. Typically, unless otherwise stated, we used an MD time step of $\delta t = 0.002$ in reduced time units and reduced inverse temperature $\beta = 100$.

3. Results and Discussion

Increasing h_X increases $\langle \chi \rangle$ locally. Most of this contribution comes from the softest non-affine modes, corresponding to $\mu = 1, 2$ (Figure 1). Note that any linear combinations of these modes are also degenerate and so the direction of the modulation wavenumber, with magnitude $\chi^{-1/2}$, varies in space pointing randomly in all directions consistent with crystal symmetry. This modulation is incompatible with global, crystalline order and therefore remains a localised (but *transient*) distortion of the lattice. We now study the consequences of enhancing the probability of *all* non-affine modes using an external field.

An advantage of studying the properties of a solid using a harmonic approximation is the possibility of obtaining exact results *even in the presence of the non-affine field h_X*. Indeed, the complete statistical mechanics of this system can be obtained analytically (apart from numerical integrals and Fourier transforms) as long as the periodic crystalline phase is stable.[18–20] In order to understand how crystal properties are affected by the non-affine field, h_X, we calculate the Hessian $\mathcal{D}(\mathbf{R}, \mathbf{R}') = \partial^2 \mathcal{H} / \partial \mathbf{u}(\mathbf{R}) \partial \mathbf{u}(\mathbf{R}')$. A Fourier transform then yields the dynamical matrix, whose eigenvalues are the phonon dispersion curves.

For convenience of representation we write the dynamical matrix as a sum of two terms $\mathcal{D}(\mathbf{q}) = \mathcal{D}_{\mathrm{harm}} + \mathcal{D}_X$, where the first term $\mathcal{D}_{\mathrm{harm}}$ corresponds to the purely harmonic part of (2) and the second term, $\mathcal{D}_X$ corresponds to the interaction arising due to the nonaffine field $(= -h_X N X)$. The harmonic part of the dynamical matrix[22] is given by,

$$\mathcal{D}_0 = k \begin{pmatrix} 3 - 2\cos(q_x) - \cos\left(\tfrac{1}{2}q_x\right)\cos\left(\tfrac{\sqrt{3}}{2}q_y\right) & \sqrt{3}\sin\left(\tfrac{1}{2}q_x\right)\sin\left(\tfrac{\sqrt{3}}{2}q_y\right) \\ \sqrt{3}\sin\left(\tfrac{1}{2}q_x\right)\sin\left(\tfrac{\sqrt{3}}{2}q_y\right) & 3\left[1 - \cos\left(\tfrac{1}{2}q_x\right)\cos\left(\tfrac{\sqrt{3}}{2}q_y\right)\right] \end{pmatrix} = k \begin{pmatrix} 3 - 2\mathcal{A}_1 - \mathcal{A}_2 & \sqrt{3}\mathcal{A}_3 \\ \sqrt{3}\mathcal{A}_3 & 3 - 3\mathcal{A}_2 \end{pmatrix},$$

(3)

procedures explained in detail in Refs.[18] and[19] and will not be repeated here.

where k and l are the spring constant and the lattice parameter of the reference harmonic lattice with q_x and

q_y being the orthogonal components of the wave vector **q**. The second term of the dynamical matrix, $\mathcal{D}_X$ can be derived from the global non-affinity parameter X. The individual components of $\mathcal{D}_X$ may be represented as

$$\mathcal{D}_X^{\nu\mu} = -h_X N \sum_j \frac{\partial^2 X}{\partial u_{\mu j}\partial u_{\nu i}} e^{-iq.(\mathbf{R}_j - \mathbf{R}_i)}.$$

Here $\mathbf{R}_j$ represents the lattice positions of all the neighbouring particles lying within the interaction volume of the particle with reference $\mathbf{R}_i$ and $u_{\mu i}$ with $\mu = x, y$ represents the x and y components of the displacement vectors of the particles. Taking double derivatives of X and performing the sum over j leads to the final expression for $\mathcal{D}_X$,

$$\mathcal{D}_X = -2\,h_X\,\mathcal{A}_X \begin{pmatrix} 1 & 0 \\ 0 & 1 \end{pmatrix}$$

with

$$\mathcal{A}_X = \frac{1}{6}\left\{ [60 - 28\cos(q_x l) \right.$$
$$-56\cos\left(\frac{q_x l}{2}\right)\cos\left(\frac{q_y\sqrt{3}l}{2}\right)\Bigg]$$
$$+\left[4\cos(2q_x l) + 8\cos(q_x l)\cos(q_y\sqrt{3}l)\right]$$
$$+\left[8\cos\left(\frac{q_x 3l}{2}\right)\cos\left(\frac{q_y\sqrt{3}l}{2}\right)\right.$$
$$\left.\left. +4\cos(q_y\sqrt{3}l)\right]\right\}.$$

Note that the leading order term in $\mathcal{A}_X(q)$ is of order $\mathcal{O}(q^4)$, so that h_X does not contribute to the speed of sound or to the elastic constants.

Assembling all terms, the full dynamical matrix in the presence of the nonaffine field is therefore given by,

$$\mathcal{D} = k\begin{pmatrix} 3 - 2\mathcal{A}_1 - \mathcal{A}_2 - \frac{2h_X}{k}\mathcal{A}_X & \sqrt{3}\mathcal{A}_3 \\ \sqrt{3}\mathcal{A}_3 & 3 - 3\mathcal{A}_2 - \frac{2h_X}{k}\mathcal{A}_X \end{pmatrix}$$

The phonon dispersion curves shown in Figure 2 are obtained by diagonalising $\mathcal{D}$. The eigenvalues, which correspond to the phonon frequencies $\omega(q)$, are given by,

$$\omega^2(q) = 3k - k\mathcal{A}_1(q) - 2k\mathcal{A}_2(q) - 2h_X\mathcal{A}_X(q)$$
$$\pm k\left[(\mathcal{A}_1(q) - \mathcal{A}_2(q))^2 + 3\mathcal{A}_3^2(q)\right]^{\frac{1}{2}}.$$

The phonon density of states is then evaluated numerically in the usual manner,[23] by counting the number of q values within the Brillouin zone which correspond to the same value of ω. The analytically obtained phonon dispersion curves $\omega_s(\mathbf{q})$ are shown in Figure 2a. The

limiting behaviour of $\omega_s(\mathbf{q})$ as $q \to 0$ *is independent of* h_X. This implies that, to leading order, h_X does not change any of the mechanical properties of the crystalline solid, nor does it introduce any stresses while enhancing non-affinity.

Increasing h_X leads to softening of certain phonon modes. While the $\mathbf{q} \to 0$ portion of the dispersion curves remain unaffected, phonon modes at intermediate and large $\mathbf{q}$ are softened. At large $\mathbf{q}$ near the zone boundary at the high symmetry M point, the phonon mode becomes soft and $\omega(\mathbf{q}) \to 0$ as h_X is increased. Inspection of the eigenvectors associated with this mode reveals that these are identical to the non-affine mode $\mu = 3$ (see Figure 1). The phonon density of states (DOS) $g(\omega) = \sum_s \int_{BZ} d\mathbf{q}\,\omega_s(\mathbf{q})\,\delta[\omega - \omega_s(\mathbf{q})]$ is shown in Figure 2b for the same values of h_X. The DOS shows a prominent shift towards $\omega = 0$ as h_X increases.

A similar shift of the DOS to small ω is a well-known consequence of introducing disorder in crystals.[14] Note that in our calculations, crystal periodicity and homogeneity is maintained. Therefore it is surprising that a similar effect is seen even in the absence of disorder. This supports our contention that this shift is due to the enhancement of non-affine fluctuations. Disorder makes these fluctuations more predominant and may lead to a broadening of the peak. We return to this question at the end of this section.

In Figures 3 and 4 we compare analytic results for the spatial non-affine correlation function with those obtained from MD calculations. The spatio-temporal correlation functions were obtained analytically as in Ref.[19] For each of these correlation functions we have obtained correlation lengths ξ_χ and times τ_χ, which are also shown. For the values of h_X where MD results corresponding to the homogeneous crystal are available, our calculations show excellent agreement with simulations. While instantaneous configurations show strong local variations of χ, these average out in time and the crystal remains homogeneous (see Figure 5a). Our results therefore show that quasi localised modes,[9] or soft spots,[6] may not be directly responsible for Boson peak like phenomena, echoing some of the conclusions of Refs.[14–16]

At larger values of h_X, both ξ_χ and τ_χ shows a divergence. Indeed all σ_μ^{-1} also vanish as $\sqrt{h_X - h_\mu^0}$ pointing to an underlying saddle-node bifurcation point beyond which a crystalline solid cannot exist. Simulations show that somewhat before this point is reached, however, the solid becomes heterogeneous through a spontaneous translational symmetry breaking dynamical transition.[26]

What happens when we, additionally, introduce disorder? We present results for our model solid using a
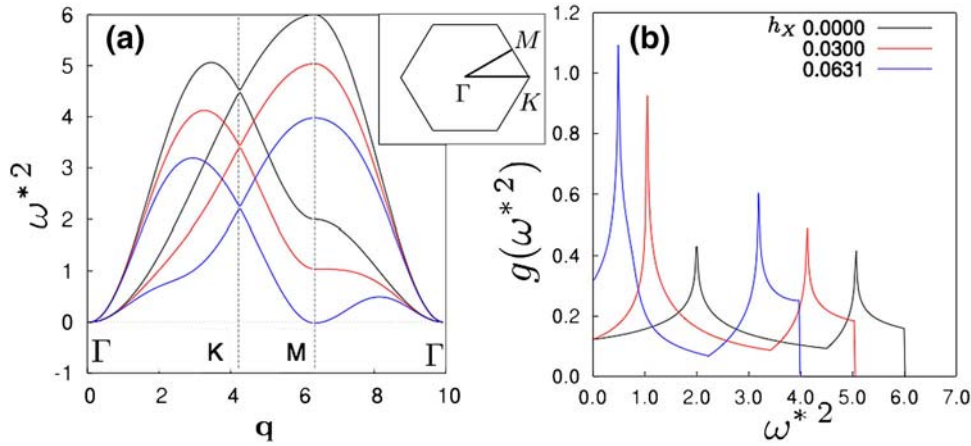
Figure 2. **a.** The phonon dispersion curves showing the square of the reduced frequency $\omega^{*2} = m\omega^2/K$ as a function of the wave number **q** along high symmetry directions (shown in the inset) for three different values of $h_X = 0$ (black), .03 (red) and .0631 (blue) a value above which the crystal becomes unstable. Both transverse and longitudinal modes are shown for each h_X. **b.** Scaled DOS calculated for the same three different values of h_X as in **a.** and indexed by the same colours. Note the softening of some modes in the dispersion curves which is reflected in the increase of the weight in the DOS for $\omega \to 0$ as h_X increases.
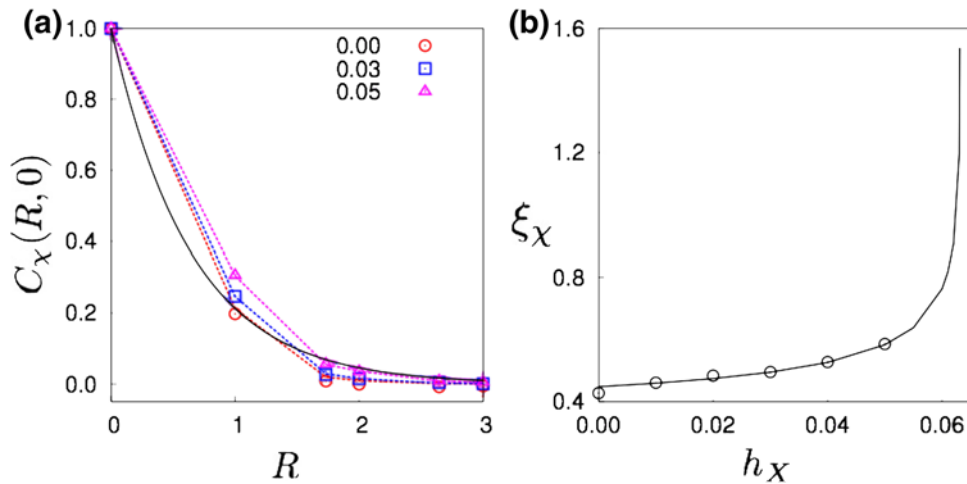

Figure 3. **a.** The radially averaged, equal time, spatial correlations, $C_\chi(R, 0)$. The points are simulation results for $h_X = 0., 0.03$ and 0.05 and the lines are from analytic calculations. **b.** Correlation lengths ξ_χ are obtained for both cases by fitting an exponential decay to the initial part of the curves (black curve, shown for $h_X = 0$). **b.** The resulting correlation length ξ_χ as a function of h_X: points simulation results and curve from analytic theory. Note the divergence as h_X increases.

simple disorder model introduced in Ref.[27] which is also similar in spirit with that of Ref.[16]. In this model, the reference configuration is maintained with the disorder appearing only in the spring constants of the bonds such that $K = 1 + \delta K$. Here, δK is taken as a random variable distributed uniformly in the range $(-K_1, K_1)$. We find that even this seemingly innocent looking disorder, when sufficiently large, is enough to make drastic changes in the structure of the non-affine modes.

This is illustrated in Figure 5 where we have plotted the probability for obtaining an eigenvalue σ for a local **PCP** matrix computed using the particle coordinates obtained from our MD simulations. For zero disorder this shows a series of well defined, but thermally broadened peaks, centred around $\sigma = \sigma_\mu$ - the eigenvalues obtained analytically for the homogeneous and periodic lattice. The peak for the largest σ_μ corresponds to dislocation precursors,[19] and is separated from the rest of the structure by a large gap where there
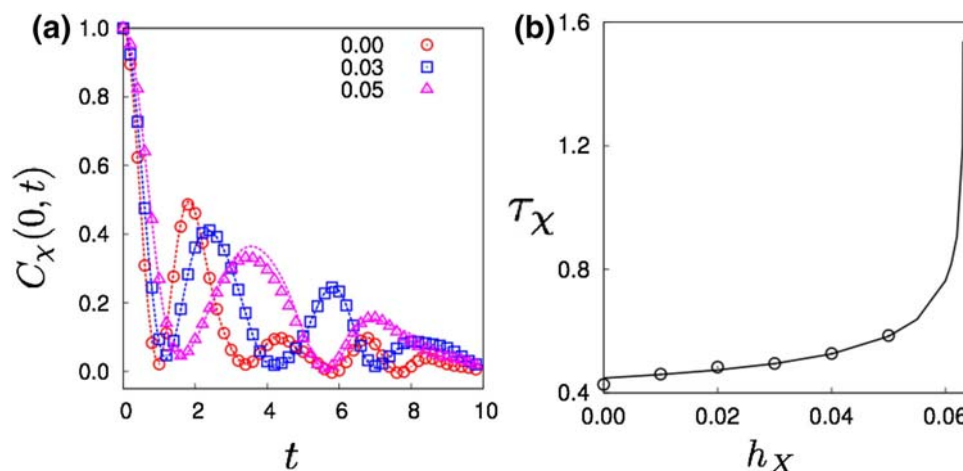
Figure 4. **a.** Temporal correlation $C_\chi(0, t)$ for the same values of h_X as in Figure 3. In this case the correlation time τ_χ is the time at which $C_\chi(0, t)$ decreases to half its initial value. **b.** The divergence of τ_χ: lines and points have same meaning as in Figure 3.
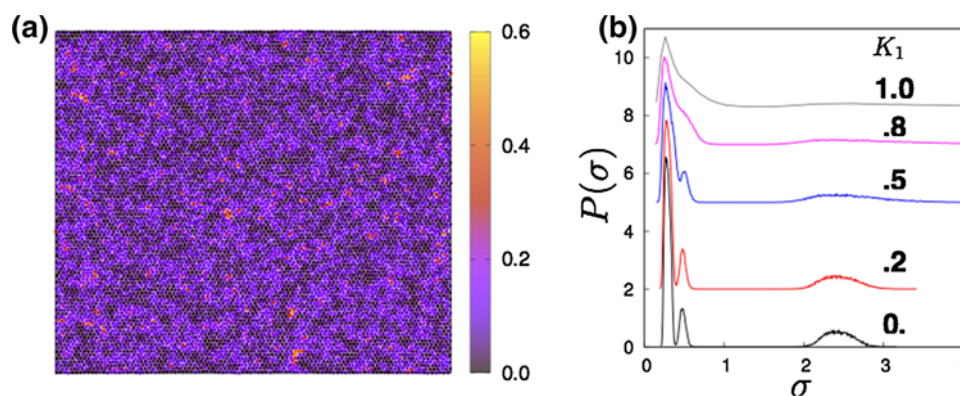
Figure 5. **a.** A typical instantaneous configuration from an MD simulation of an ordered, harmonic $N = 100 \times 100$ lattice at $h_X = 0.05$ and no disorder with the particles coloured according to the local values of χ. Note that while the distribution of χ is spatially heterogeneous, these heterogeneities average out in time. **b.** Plot of the probability distribution $P(\sigma)$ of the eigenvalues of PCP at $h_X = 0$ and for various values of disorder K_1 (see text). For the pure solid ($K_1 = 0$) the distribution has peaks centred at each $\sigma = \sigma_\mu$ with only thermal broadening. As disorder is increased, the peaks broaden and the identity of each separate non-affine mode is lost.

are no eigenvalues. As disorder increases, the once distinct, separate, non-affine modes loose their identities and the mode structure becomes more and more diffuse. Each local region now contributes a different set of vibrational modes with different frequencies thereby broadening the density of states as seen in Ref. [15].

4. Conclusions

In this paper we show that enhancing non-affine fluctuations alone using an external field is sufficient to produce an excess of low frequency vibrational modes in a crystal *without* disorder. This occurs due to a shift of the lowest van-Hove singularity of the crystal to low frequency. These results are quite similar to the findings of Ref. [16] where a similar shift was observed as an effect of disorder. In our case, the solid, on the other hand, remains ordered, homogeneity and periodicity being imposed for all our analytic calculations. We thus conclude that disorder is *a sufficient but not necessary condition* for the appearance of boson peak phenomena. Non-affine displacements, which cause a shift of the van-Hove singularity, can be enhanced either by making the crystal disordered or independently using a specific external field.

The external field h_X, nevertheless remains, at present, a mathematical device realisable only in computer simulations. However, we have mentioned in Ref.[19] how one may be able to generate such a field experimentally in a colloidal solid. Briefly, one can use video microscopy to obtain information about the current position of atoms and selectively apply appropriate forces using dynamic laser traps. In case such a feedback system is actually set up in the future, we believe that the results shown here and earlier in Ref.[19] would be valuable as a benchmark.

There are several future directions which one may explore starting from the results presented here. Firstly, a more complete study is needed to elucidate the role of quenched disorder. Specifically, the complementary question of whether Boson peak phenomena in disordered solids may be influenced by similar external fields needs to be studied. For example, one may be able to suppress non-affine displacements, calculated with respect to a suitably defined reference configuration in a disordered crystal using some $h_X < 0$. Will that also make the Boson peak decrease or even disappear? Finally we would like to extend this work to higher dimensions and towards more realistic materials.

Acknowledgements

References

1. Chaikin P and Lubensky T 1995 *Principles of Condensed Matter Physics* (Cambridge: Cambridge Press)
2. Ediger M D 2000 Spatially Heterogeneous Dynamics in Supercooled Liquids *Annu. Rev. Phys. Chem.* **51** 99
3. Binder K and Kob W 2011 *Glassy Materials and Disordered Solids: An Introduction to Their Statistical Mechanics 2011* (Singapore: World Scientific)
4. Cavagna A 2009 Supercooled Liquids for Pedestrians *Phys. Rep.* **476** 51
5. Berthier L and Biroli G 2011 Theoretical Perspective on the Glass Transition and Amorphous Materials *Rev. Mod. Phys.* **83** 587
6. Manning M L and Liu A J 2011 Vibrational Modes Identify Soft Spots in a Sheared Disordered Packing *Phys. Rev. Lett.* **107** 108302
7. Falk M L and Langer J S 2010 Deformation and Failure of Amorphous Solidlike Materials *Annu. Rev. Condens. Matter Phys.* **2** 353
8. Falk M L and Langer J S 1998 Dynamics of Viscoplastic Deformation in Amorphous Solids *Phys. Rev. E* **57** 7192
9. Shintani H and Tanaka H 2008 Universal Link Between the Boson Peak and Transverse Phonons in Glass *Nat. Mater.* **7** 870
10. Laird B B and Schober H R 1991 Localized Low-Frequency Vibrational Modes in a Simple Model Glass *Phys. Rev. Lett.* **66** 636
11. Buchenau U and Schober H R 2008 An Atomic Mechanism for the Boson Peak in Metallic Glasses *Phil. Mag.* **88** 3885
12. Ghosh A, Chikkadi V, Schall P and Bonn D 2011 Connecting Structural Relaxation with the Low Frequency Modes in a Hard-Sphere Colloidal Glass *Phys. Rev. Lett.* **107** 188303
13. Parshin D A, Schober H R and Gurevich V L 2007 Vibrational Instability, Two-level Systems, and the Boson Peak in Glasses *Phys. Rev. B* **76** 064206
14. Schirmacher W, Diezemann G and Ganter C 1999 Model Calculations for Vibrational Properties of Disordered Solids and the "boson peak" *Physica B* **263–264** 160
15. Chumakov A I et al. 2011 Equivalence of the Boson Peak in Glasses to the Transverse Acoustic van Hove Singularity in Crystals *Phys. Rev. Lett.* **106** 225501
16. Taraskin S N et al. 2001 Origin of the Boson Peak in Systems with Lattice Disorder *Phys. Rev. Lett.* **86** 1255
17. Schall P, Weitz D A and Spaepen F 2007 Structural rearrangements that govern flow in colloidal glasses *Science* **318** 5858
18. Ganguly S, Sengupta S, Sollich P and Rao M 2013 Nonaffine Displacements in Crystalline Solids in the Harmonic Limit *Phys. Rev. E* **87** 042801
19. Ganguly S, Sengupta S and Sollich P 2015 Statistics of Non-affine Defect Precursors: Tailoring Defect Densities in Colloidal Crystals Using External Fields *Soft Matter* **11** 4517
20. Mitra A, Ganguly S, Sengupta S and Sollich P 2015 Non-affine Fluctuations and the Statistics of Defect Precursors in the Planar Honeycomb Lattice *JSTAT P06025*
21. Balu R W 2012 *Introduction to the Elasticity Theory for Crystal Defects* (Cambridge: Cambridge University Press)
22. Garboczi E J and Thorpe M F 1985 Density of States for Random-central-force Elastic Networks *Phys. Rev. B* **32** 4513
23. Ashcroft N W and Mermin N D 1976 *Solid State Physics* (New York: Holt, Rinehart, and Winston)
24. Chakravarty C, Debenedetti P G and Stillinger F H 2007 Lindemann Measures for the Solid liquid Phase Transition *J. Chem. Phys.* **126** 204508
25. Frenkel D and Smit B 2002 *Understanding Molecular Simulations* (San Diego: Academic Press)
26. Ganguly S, Horbach J, Sollich P, Nath P, Karmakar S and Sengupta S 2016 Equilibrium and dynamic pleating of a crystalline bonded network arXiv:1612.00574 (to appear in *J. Chem. Phys.* 2017)
27. Didonna B and Lubensky T C 2005 Nonane correlations in random elastic media *Phys. Rev. E* **72** 66619